International Journal of Heat and Mass Transfer 52 (2009) 5525–5532

Contents lists available at ScienceDirect

International Journal of Heat and Mass Transfer

journal homepage: www.elsevier.com/locate/ijhmt

Effective thermal conductivity of various filling materials for vacuum insulation panels

Jae-Sung Kwon, Choong Hyo Jang, Haeyong Jung, Tae-Ho Song *

Department of Mechanical Engineering, Korea Advanced Institute of Science and Technology, Guseong-dong 373-1, Yuseong-gu, Daejeon, Republic of Korea

ARTICLE INFO

Article history:
Received 4 December 2008
Received in revised form 17 June 2009
Accepted 17 June 2009
Available online 27 July 2009

Keywords:
Vacuum insulation panel
Effective thermal conductivity
Filling materials

ABSTRACT

Three thermal transport mechanisms of various filling materials for Vacuum Insulation Panels (VIPs) are theoretically investigated with special emphasis on the solid conduction. As the first, the solid conductivities of porous materials such as powder, foam, fiber and staggered beam subject to external atmospheric compression are derived using simplified elementary cell models. The results show that the solid conductivities of the fiber and staggered beam insulation are lower than those of the powder and foam due to the relatively long thermal path. The second mechanism, i.e., gaseous conductivity shows the lowest for the fine powder among the considered materials due to its smallest pore size. The radiative conductivity as the last is calculated using the diffusion approximation. If radiation shields are installed for the staggered beam, the radiation effect can be lowered to a negligible order of magnitude. The predicted total effective conductivities suggest that the fiber and staggered beam structures are promisingly proper filling materials for VIPs.

1. Introduction

A recent survey shows that 48% of the total energy consumption in the USA is made in buildings [1]. Needless to say, high performance thermal insulation is increasingly required to reduce energy consumption and/or to save valuable space. A superior thermal insulation can be achieved by so called vacuum insulation panel (VIP). Evacuated insulation enables a VIP to have about 10 times higher thermal resistance than the conventional insulators such as polystyrene or polyurethane foams. Similarly to a conventional Dewar flask or Thermos flask, a VIP makes use of vacuum to suppress the heat transfer due to gaseous conduction. While the Dewar flask has cylindrical shape made of glass or stainless steel wall, the flat type VIP must have a core material which withstands the atmospheric pressure and a gas-tight envelope maintaining the inside vacuum level. The core material has to be porous to easily evacuate and to have minimum conduction heat transfer effect. For this reason, materials in the form of powders, foams and fibers are used as the VIP core material [2]. In addition to the above conventional insulation materials, artificial structures such as staggered beams or honeycomb are proposed for the VIP's filling material [3,4].

Thermal transport in a VIP occurs via solid conduction, gaseous conduction and radiation. The solid conduction depends on the structure and material properties of the core. The gaseous conduction by residual gases depends on the gas pressure which increases with time by infusion of atmospheric gases and outgassing of the inner material. Thermal radiation depends on the structure and optical properties of the core. The total effective conductivity k_{eff} of the VIP can be determined by summation of the solid conductivity k_s, the gaseous conductivity k_g and the radiative conductivity k_r as

$$k_{eff} = k_s + k_g + k_r. \quad (1)$$

Separate study of each contribution is required to improve the thermal insulation performance of the VIP. However, experimental separate measurement of these contributions is not easy because any of them cannot be fully eliminated. So, a theoretical study on the separate heat transfer mechanisms of the VIP is very instrumental for improving the thermal performance of a VIP.

Numerous studies on the heat transfer mechanisms of the non-evacuated conventional insulators have been conducted. For instance, Chan and Tien [5] analyzed conductance of packed spheres in vacuum. Also, an analytical model for predicting the effective thermal conductivity of packed beds of spheres is developed by Turyk and Yovanovich [6]. Thermal transport mechanisms in closed-cell foam insulations are described by Kuhn et al. [7]. For the fibrous insulation, heat transfer mechanisms are calculated theoretically and compared with the experimental data by Bankvall [8]. However, few studies on the thermal transport mechanisms of the various evacuated insulators are found in the literature.

The aim of this paper is a theoretical investigation of the thermal transport mechanisms with special emphasis on the solid

* Corresponding author. Tel.: +82 42 350 3032; fax: +82 42 350 3210.
E-mail address: thsong@kaist.ac.kr (T.-H. Song).

0017-9310/$ - see front matter © 2009 Elsevier Ltd. All rights reserved.
doi:10.1016/j.ijheatmasstransfer.2009.06.029

Nomenclature

b	width of staggered beam, m
e	specific extinction coefficient, m^2/kg
e_λ	spectral specific extinction coefficient, m^2/kg
E	Young's modulus of elasticity, N/m^2
E_R	Rossseland mean extinction coefficient, m^{-1}
F	external force, N
h	height of staggered beam, m
k	thermal conductivity, W/m K
L	length of elementary cell of foam, m
M	molecular weight of gas, g/mol
n	refractive index
P	pressure, N/m^2
q	heat flux, W/m^2
r	radius, m
R	thermal resistance, K/W
S	conduction shape factor
t	thickness, m
T	temperature, K
W	distance between beams, m
Z	figure of merit, MPa m K/W

Greek symbols

α	accommodation factor
γ	specific heat ratio
δ	distance between fibers, m
θ	tilted angle of fibers, radian
λ	mean free path, m
ν	Poisson's ratio
Π	porosity
ρ	density, kg/m^3
σ	Stefan-Boltzmann constant
σ_t	tensile strength, N/m^2
ϕ_τ	pore size, m

Subscripts

atm	atmospheric
c	contact
eff	effective
f	fiber
g	gaseous
m	mean
p	powder
r	radiative
s	solid
st	strut
th	thermal

conductivity for various VIP core structures including powder, foam, fiber and the staggered beam core. The solid conductivity is determined via a theoretical model. The gaseous and the radiative conductivities are derived by using separate theoretical models. With the above calculated results, the three heat transfer effects in VIPs are scrutinized in depth.

2. Solid conduction

2.1. Powder insulation

Powders are often used as the filling material in vacuum for cryogenic applications. Materials such as perlite or silica are formed into fine granular particles. It is difficult to completely describe the effective solid conductivity due to the randomness of the packed bed structure. Instead, two cases are investigated using two different models. Firstly, a loose simple cubic arrangement of packed spheres is considered as a typical model (Fig. 1(a)). And then, a hexagonal close-packed model is analyzed (Fig. 1(b)).

The contact resistance can be calculated using Hertz contact theory [9]. The contact modulus defining the elastic properties of spheres 1 and 2 is given by

$$\frac{1}{E_0} = \frac{1-\nu_1^2}{E_1} + \frac{1-\nu_2^2}{E_2}, \tag{2}$$

where E is Young's modulus and ν is Poisson's ratio. A radius r_0 named as the relative contact radius is expressed by summation of each curvature;

$$\frac{1}{r_0} = \frac{1}{r_1} + \frac{1}{r_2}. \tag{3}$$

The true radius of contact circle r_c is then

$$r_c = \left(\frac{3Fr_0}{4E_0}\right)^{1/3}, \tag{4}$$

where F is the external force loaded on the sphere.

Consider the simple cubic model of Fig. 1(a). Since it can be assumed that the contact radius is very small compared to the size of the sphere, the conduction may be treated using the conduction shape factor [10] involving a disk of radius r_c placed on semi-infi-

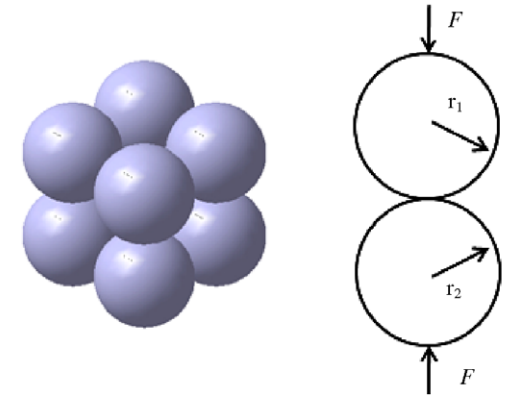

(a) simple cubic model

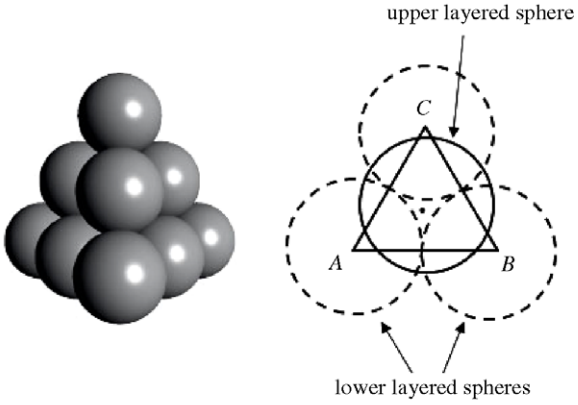

(b) hexagonal close-packed model

Fig. 1. Regularly packed sphere models.

nite medium. The heat flux from sphere 1 to sphere 2 can be written by

$$q = k_{p,1}S_1(T_1 - T_c) = k_{p,2}S_2(T_c - T_2), \tag{5}$$

where k_p is the thermal conductivity of the sphere, T is the temperature of the sphere and the subscripts 1,2 and c express the spheres 1, 2 and the contact point, respectively. Since $S = 4r_c$, Eq. (5) leads to

$$q = 4r_c\left(\frac{1}{k_{p,1}} + \frac{1}{k_{p,2}}\right)^{-1}(T_1 - T_2). \tag{6}$$

For two identical spheres of same material and size, the thermal resistance can be obtained using Eqs. (4) and (6) as

$$R_{th} = \left[k_p r\left(\frac{24P_{atm}(1-\nu^2)}{E}\right)^{1/3}\right]^{-1}, \tag{7}$$

where P_{atm} is the atmospheric pressure exerting on the sphere. The effective thermal resistance for a height of $2r$ and area $4r^2$ can be defined by

$$R_{th} = \frac{1}{2k_{s,powder}r}. \tag{8}$$

Therefore, the effective solid conductivity $k_{s,powder}$ of the simple cubic model of powders can be obtained by

$$k_{s,powder} = k_p\left(\frac{3(1-\nu^2)P_{atm}}{E}\right)^{1/3}. \tag{9}$$

It is noteworthy that it is independent of the powder size. For a silica powder with $E = 73$ Gpa, $\nu = 0.17$ and $k_p = 1.38$ W/m K, one gets $k_{s,powder} = 0.0219$ W/m K using the above equation.

For identical packed spheres, the maximum density occurs at hexagonal close-packed arrangement (Fig. 1 (b)). This model, thus, yields the upper limit of the effective thermal conductivity. Consider the unit cell structure shown in Fig. 1 (b). The spheres A, B and C are placed in the lower layer, the sphere D is in the upper layer. Because the external load applied to ΔABC is equally distributed on the three contact points, the force exerted on the one of the contact points is given as

$$F_c = \frac{1}{3}P_{atm}\Delta ABC\frac{\sqrt{3}}{\sqrt{2}}. \tag{10}$$

Heat flux from the upper sphere D to the lower spheres A, B, and C through three contact points can be expressed as

$$q = 6r_c k_p(T_D - T_A) = k_{s,powder}\frac{\sqrt{3}\Delta ABC}{2\sqrt{2}r}(T_D - T_A). \tag{11}$$

So, the effective solid conductivity of hexagonal close-packed spheres is given as

$$k_{s,powder} = k_p\left(\frac{96(1-\nu^2)P_{atm}}{E}\right)^{1/3}. \tag{12}$$

For the same silica powder values as in the simple cubic model, one gets $k_{s,powder} = 0.0634$ W/m K. This is the upper bound of the effective solid conductivity of silica powders.

The analysis introduced here is similar to that of Chan and Tien [5], except that they solved the conduction equation in the sphere. For the silica powder, they present results as $k_{s,powder} = 0.0206$ W/m K and 0.0412 W/m K in the simple cubic model and hexagonal closed-packed model, respectively. Though small, this discrepancy remains to be treated in a further experimental study.

In the meanwhile, Fricke et al. [11] reports the solid conductivity of evacuated silica powders as $k_{s,powder} \approx 0.005$ to 0.01 W/m K after excluding other effects from the experiments. This value is significantly lower than the calculated results using the two models. This discrepancy is thought to be due to the higher porosity than these models and the effect of surface roughness. The porosities of the simple cubic model, hexagonal close-packed model and the sample used in [11] are 0.48, 0.26 and 0.84, respectively. When particles of uneven sizes are packed in a random manner, there are more cavities than these two models. This lowers the effective conductivity. Indeed, it is reported that the solid conductivity of randomly packed powders depends on the porosity as [12]

$$k_s \sim (1 - \Pi)^m, \tag{13}$$

where Π is the porosity and $m \approx 1$ to 2. In addition, while the sphere surface is assumed as perfectly smooth in the Hertz contact theory, real particles have random rough surfaces. When random rough surfaces are in contact each other, real contact occurs at peak of the surface called microcontacts. This microcontact is thought to cause additional thermal resistance [13]. The exact relation of k_s vs. Π, however, may be found when extensive experimental data are accumulated.

2.2. Foam insulation

Foam insulations are the most widely used ones due to the low cost and ease of production. They are generally classified into closed-cell and open-cell foams. The former has cell walls to trap low thermal conductivity gas inside. Conduction of heat occurs through the struts and the cell wall. The open-cell foams such as rigid polyurethane are generally used for the VIP core material thanks to ease of evacuation. Since this research is confined to VIP, only the open-cell type is considered and thus, the cell wall effect is not considered. A simple cubic model as an idealized cell geometry is shown in Fig. 2. Consider only one quarter of the cubic cell as a symmetric elementary cell. It is assumed that the foam is rigid so that the buckling of the strut due to compressive force does not occur. If the heat flow path is parallel to the vertical line of the elementary cell, the total thermal resistance comprises four components: (a) resistance in the vertical strut, (b) one in the horizontal strut, (c) one in the gas between the horizontal struts, and (d) one in the void space. These four resistances and the total resistance can be expressed, respectively, as

$$R_1 = \frac{L}{k_{st}t^2}, \quad R_2 = \frac{2}{k_{st}(L-2t)}, \quad R_3 = \frac{2}{k_g t},$$
$$R_4 = \frac{4L}{k_g(L-2t)^2}, \quad R_{th} = \frac{4}{k_{s,foam}L}, \tag{14}$$

where k_{st} is the solid conductivity of the strut, k_g is the thermal conductivity of gas filling void space, L is the length of a cell and t is the thickness and height of a strut. Thermal resistance network for the element cell is shown in Fig. 3. So, the effective thermal conductivity can be derived as

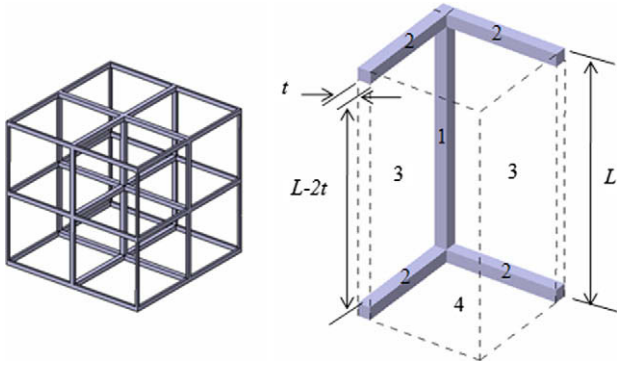

Fig. 2. Simple cubic model of the open-cell foam.

$$k_{s,foam} = \frac{4k_{st}t^2 + k_g(L-2t)^2}{L^2} + \frac{4k_{st}k_g(L-2t)t}{2Lk_gt + Lk_{st}(L-2t)}. \quad (15)$$

This equation expresses the effects of gaseous conduction as well as the solid conduction. If the foam is assumed to be completely evacuated, the gaseous conductivity can be neglected by setting $k_g = 0$. Then, the effective solid conductivity of the foam is given by

$$k_{s,foam} = \frac{4k_{st}t^2}{L^2}. \quad (16)$$

The porosity is defined as the ratio of void volume to the bulk volume. For the one quarter cell under consideration, the porosity Π can be written as

$$\Pi = 16\left(\frac{t}{L}\right)^3 - 12\left(\frac{t}{L}\right)^2 + 1. \quad (17)$$

If the porosity of the foam insulator is given, this equation can be solved for t/L. For example, typical polyurethane foam values like $k_{st} = 0.26$ W/m K and $\Pi = 0.94$ give $t/L = 0.07$ and $k_{s,foam} = 0.005$ W/m K. This is in a good accordance with the result from the following approximate equation reported by Schuetz and Glicksman [14];

$$k_{s,foam} = \frac{1}{3}k_{st}(1-\Pi), \quad (18)$$

as this equation yields, $k_{s,foam} = 0.0052$ W/m K. Typical values of evacuated foams are also reported as $k_{s,foam} \approx 0.003$ to 0.007 W/m K following Fricke et al. [15].

2.3. Fibrous insulation

Fibrous materials are widely used for its light weight and high temperature durability. According to Fricke et al. [16], the effective conductivity is dependent on a number of parameters: solid conductivity of the fiber material, Young's modulus, porosity, imposed pressure and fiber orientation. The fibers are normally oriented randomly with respect to the main heat flow direction. Consider a model consisting of plane layers of equally spaced parallel fibers placed perpendicular to the main heat flow direction (see Fig. 4). The circular cylinder fibers of the first layer (the lowest ones in the figure) and those of the second layer are inclined at angle θ. The fibers in the third layer are assumed to be ideally placed half pitch with respect to the first layer ones to maximize the heat flow path. The elementary conduction path (the dotted parallelogram in the figure) is considered for analysis. It consists of the two half

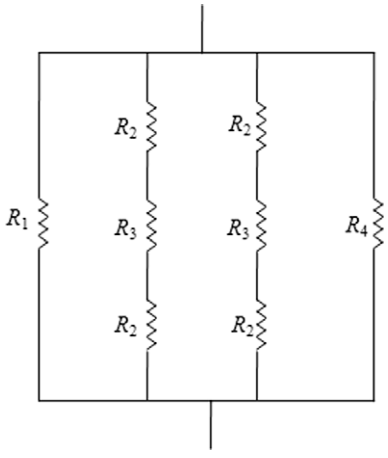

Fig. 3. Thermal resistance network of the elementary cell.

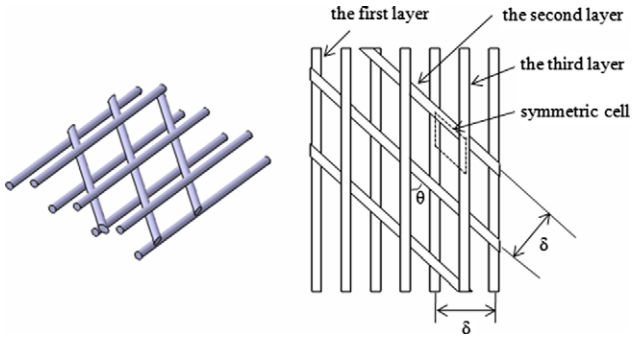

Fig. 4. A simple model of the fibrous insulation.

cylinder rods and two contact points in series and the total thermal resistance can be presented as

$$R_{th} = \frac{1}{2k_fr_{ct}} + \frac{2\delta}{k_f\pi r_f^2\sin\theta}, \quad (19)$$

where δ is the distance between the fibers within a layer and r_f is the radius of the fiber. The total thermal resistance in terms of $k_{s,fiber}$ is also written as

$$R_{th} = \frac{4r_f}{k_{s,fiber}(\delta^2/4\sin\theta)}. \quad (20)$$

As the two identical cylinders are in contact at angle θ, the equivalent relative radius of contact is given as [9]

$$r_0 = \frac{\sqrt{2}r_f}{1-\cos 2\theta}. \quad (21)$$

When there is no deflection of the fiber, the porosity is implicitly expressed by

$$\frac{r_f}{\delta} = \frac{2}{\pi}(1-\Pi). \quad (22)$$

Using Eqs. (4), (19)–(22), the effective thermal resistance can be derived as

$$k_{s,fiber} = 16k_f\left[\left(\frac{\sqrt{2}\pi^4E}{24P(1-\Pi^4)(1-\nu^2)}\right)^{1/3} + \frac{\pi^2}{4(1-\Pi)^3\sin^2\theta}\right]^{-1}. \quad (23)$$

This expression is very similar to the equation reported in the literature [16]. It is interesting to note that $k_{s,fiber}$ is maximum at $\theta = \pi/2$. For real layers, however, θ varies in a random manner. The mean effective thermal conductivity with random orientation θ can be calculated numerically by the following arithmetic mean equation over N variations of θ by $\Delta\theta$;

$$\overline{k_{s,fiber}(\theta)} = \frac{1}{N}\sum_{i=1}^{N} k_{s,fiber}\left(\frac{i}{N}\Delta\theta\right). \quad (24)$$

The calculation result for a glass fiber ($E = 72.4$ Gpa, $\nu = 0.2$, $k_f = 1.3$ W/m K, $\Pi \approx 0.9$) shows $k_{s,fiber} = 0.0021$ W/m K. This is in good accordance with the approximate result $k_{s,fiber} = 0.0024$ W/m K reported by Fricke et al. [16]. Fricke et al. [15] also report typical value of the pressure loaded fibers as $k_{s,fiber} \approx 0.001$ to 0.003 W/m K.

2.4. Staggered beam structure

Filling materials of VIPs must withstand the compression by the external atmospheric pressure and have minimum solid conduction. To reduce the solid conduction, the thermal conduction

path should be tortuously long. Considering these requirement, the staggered beam structure as shown in Fig. 5 has been proposed by Kawaguchi and Nagai [3]. The parallel beams having rectangular cross-section in the first layer are placed at right angles to those of the second layer. Those in the third layer are placed half pitch to the first layer ones. This staggering alignment is the same as the model of Fig. 4 except that the cross-section is rectangular and the angle θ is fixed at $\pi/2$. Taking the rectangular cross-section is advantageous to increase the beam stiffness, and indeed, taking an I-shaped cross-section would further improve that.

Considering two beam layers as in Fig. 5, the thermal resistance can be expressed by

$$R_{th} = \frac{W}{2k_b bh}, \tag{25}$$

where k_b is the solid conductivity of the beam, b is the width of the beam, h is the height of the beam and W is the distance between the beams in the layer. Consider the strength of a beam in the second layer. When the external force $P_{atm}W^2$ is applied on the center of the second layer beam, the following equation must be satisfied to avoid fracture;

$$\frac{3P_{atm}}{4\sigma_t} \le \frac{bh^2}{W^3}, \tag{26}$$

where P_{atm} is the atmospheric pressure and σ_t is the tensile strength of the beam. Using Eqs. (25) and (26), the effective solid conductivity for the staggered beam structure of thickness $2h$ is given as (neglecting beam deflection)

$$k_{s,beam} = 3k_b \frac{P_{atm}}{\sigma_t}. \tag{27}$$

This shows that the material must have greater σ_t/k_b for better insulation. We may call this number 'figure of merit' Z as

$$Z = \frac{\sigma_t}{k_b}. \tag{28}$$

Various materials are examined. In general, metals have lowest Z (from about 10 to 120 MPa m K/W), ceramic and glasses are in the middle (90–200 MPa m K/W) and plastics and polymers exhibit the best performance (150–500 MPa m K/W). The highest Z is for polyimide, within the author's search. Considering price and manufacturability, polycarbonate is taken as the beam material. For this, Eq. (27) gives $k_{s,beam}$ = 0.0009 W/m K using σ_t = 65 MPa, k_b = 0.2 W/m K. Note that Eq. (27) shows there is no difference in $k_{s,beam}$ by increasing W and thus b and/or h.

Consider a case of the staggered oblique alignment (upper parallel beams are rotated at angle θ) like the fibrous insulation model. The thermal resistance decreases with increasing θ due to the extended thermal path, but stress loaded on the beam is increased with angle θ. Therefore, the effective solid conductivity is independent of angle θ.

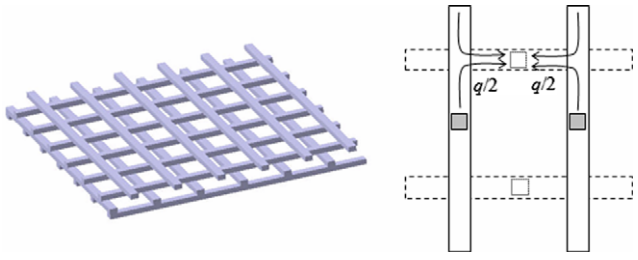

Fig. 5. Staggered beam structure.

3. Gaseous conduction

Thermal transport in VIPs also occurs due to residual thin gas in the internal space. Thermal conductivity of gas is independent of pressure as far as the gaseous conduction may be treated as a continuum. This phenomenon is the result of the inverse relation between pressure and mean free path [17]. However, thermal conduction by gas is significantly reduced when the mean free path of gas molecules is about equal to or greater than the distance over which heat is transported. The mean free path $\lambda(m)$ for air, at room temperature can be written as [17]

$$\lambda = \frac{6.65 \times 10^{-3}}{P}, \tag{29}$$

where P is the pressure in Pa(N/m^2). If the pore size of the VIP core material is known, the pressure level in which gaseous conduction is significantly lowered can be determined using Eq. (29). For a polyurethane foam VIP with a pore size of about 100 μm, this corresponds to a pressure of 66.5 Pa.

A theory of gaseous thermal conduction in rarefied gas has been developed by Smoluchowski [18]. It is based on the concept of a temperature jump or discontinuity which is analogous with the phenomenon of viscous slip. For two parallel plane surfaces separated by a distance ϕ, the energy flux q between the surfaces at low pressure is given by

$$q = \frac{k_{g0}}{\phi + 2\beta}(T_1 - T_2), \tag{30}$$

where k_{g0} is the thermal conductivity of the free gas. And β is given as [19]

$$\beta = \left(\frac{9\gamma - 5}{2\gamma + 1}\right)\left(\frac{2 - \alpha}{\alpha}\right)\lambda, \tag{31}$$

where γ is the specific heat ratio of gas and α is the accommodation coefficient. Common gases have α between 0.7 and 1 at room temperature [20]. Using Eq. (29) and γ = 1.4 and α = 0.8 for air at 25 ℃, Eq. (31) can be rewritten as $\beta = 0.016/P$. So, the gaseous thermal conductivity can be derived by Fourier's heat conduction equation which is analogous to Eq. (30);

$$k_g = \frac{k_{g0}}{1 + \frac{0.032}{P\phi}}. \tag{32}$$

The gaseous thermal conductivities with different pore sizes are shown as a function of gas (25 ℃ air) pressure in Fig. 6. It is shown that the smaller pore-sized material is less sensitive to pressure increases in vacuum compared to the larger pore-sized material. For example, the calculated gaseous conductivities at the pressure of 10 Pa are 7.88×10^{-4}W/m K and 8.10×10^{-5}W/m K with ϕ = 100 μm and ϕ = 10 μm, respectively. So, the gaseous conduction in the material having pore size of ϕ = 10 μm can be neglected at the pressure of 10 Pa.

4. Radiative conductivity

Radiation at low pressure is another important heat transfer mechanism for VIPs. Radiation from a hot surface is attenuated via scattering and absorption/emission of the core structure. Two approaches are generally considered to describe the radiation heat transfer in thermal insulations structures, following Petrov [21].

The first approach is based on the radiative transfer equation (RTE). It can be solved numerically if the spectral and temperature dependencies of the absorption coefficient and refractive index are known. The second one is the use of diffusion approximation which is the most frequently used method. This has the advantage of simplicity but the application is limited to the case of optically

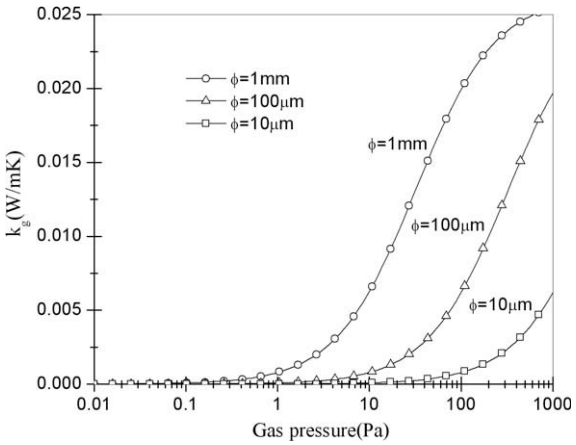

Fig. 6. Gaseous conductivity with different pore sizes as a function of gas pressure.

thick medium. According to the diffusion approximation, the radiative conductivity within an optically thick specimen for a mean temperature T_m is given by [22]

$$k_r = \frac{16n^2\sigma T_m^3}{3E_R(T_m)}, \tag{33}$$

where n is the index of refraction, σ is the Stefan-Boltzmann constant. The Rosseland mean extinction coefficient E_R which is correlated with the density ρ and mass specific extinction $e(T_m)$ can be expressed as

$$E_R(T_m) = e(T_m)\rho. \tag{34}$$

As a first step to determine E_R, the spectral mass specific extinction e_λ is measured from IR extinction over the wavelength range 2–40 μm. Then, $e(T_m)$ can be obtained from proper weighted averaging of e_λ over the thermal spectrum.

Typical values of $e(T_m)$ for foams are in the range from 30 to 60 m^2/kg at 300 K [7]. In case of rigid open-cell foams, the relationship between density and the extinction coefficient is proposed by Tao et al. [23] as follows:

$$E_R(T_m) = 42.038\rho + 121.55. \tag{35}$$

For the foam insulation with $\rho = 70$ kg/m^3, the radiative conductivity $k_r = 0.0027$ W/m K is obtained at 300 K.

For glass fibers at 300 K with fiber diameters 0.5 and 0.7 μm, parameters for Eq. (34) are $e = 60$ and 76 m^2/kg, respectively, following Caps et al. [24]. For the fibrous insulation with $\rho = 250$ kg/m^3, $e = 50$ m^2/kg is reported by Mathes et al. [25]. Using this data, the radiative conductivity of the fibrous insulation with density of $\rho = 250$ kg/m^3 is obtained as $k_r = 0.0007$ W/m K. Caps et al. [26] also report, for powder materials, $e = 20$ m^2/kg for $\rho = 180$ kg/m^3. In case of the highly dense powder with $\rho = 1100$ kg/m^3, $e = 36$ m^2/kg is reported by Wang and Tien [27]. Using this value, radiative conductivity $k_r = 0.0002$ W/m K is given. Due to the lack of published extinction coefficient for the staggered beam, staggered beams are treated as fibers having diameter larger than wavelengths of the order of 10 μm. For these fibers which are enclosed between two surfaces, the radiative conductivity is given as [28]

$$k_r = \frac{4\sigma T_m^3[2r_f/(1-\Pi)]t_{core}}{t_{core} + [2r_f/(1-\Pi)]\left(\frac{1}{\varepsilon}-1\right)}, \tag{36}$$

where r_f is the radius of the fiber, t_{core} is the thickness of the VIP and ε is the emissivity of the surfaces. For $r_f = 1$ mm, $t_{core} = 1$ cm, $\Pi = 0.84$ and $\varepsilon = 0.8$, radiative conductivity of staggered beam $k_r = 0.033$ W/m K is obtained. It is readily seen that k_r contributes significantly to the total effective conductivity. Radiation, thus, has to be treated with a special attention.

A promising method of reducing the radiative transfer is to install reflective surfaces in the gap. They function as radiation shields. An advantage of the staggered beam VIP is the possibility of installing multi-layered radiation shields between the beam layers (see Fig. 7). A very thin aluminum foil (6 or 7 μm) is generally acceptable thanks to the low emissivity and cheap price. The thermal resistance across the thin aluminum foil in the central part of VIP can be neglected, since the foil thickness is much smaller than the VIP thickness. However, the vertical direction conduction through the envelope (especially through its aluminum layer) may be a serious problem, although it is not treated here. Suffice it to mention that, for the central part, the thermal conduction effect by the aluminum foil shield can be ignored.

When the gap between the shields is as small as micro-meter, there exists evanescent wave in the gap which complicates the analysis significantly. Yoon and Song [29], after performing the analysis, conclude that the radiative transfer may be treated using simple ray theory if the gap is more than 5 μm at room temperature. Analysis here is limited to such case. It is also assumed that the radiation attenuation by staggered beam structure itself can be ignored. Considering only two layers of the beam, two radiation gaps are made by the inter-surface. The radiative conductivity of staggered beam structure including N gaps can be written as

$$k_r = \frac{t_{core}\sigma T_m^3}{N\left(\frac{2}{\varepsilon}-1\right)}, \tag{37}$$

where t_{core} is the thickness of the VIP, T_m is the average temperature within the VIP and ε is the emissivity of the surface. For $t_{core} = 4$ mm, $N = 2$, $\varepsilon = 0.04$ (aluminum foil at 300 K) and $T_m = 300$ K, radiative conductivity is obtained as $k_r = 0.0003$ W/m K. Note that k_r has decreased to a negligible order of magnitude.

5. Practical examples and discussions

The theoretically calculated solid conductivities k_s of the various insulation materials for VIP are shown in Table 1. Note that the actual measurement reports exceptionally smaller solid conductivity for spherical powder, and thus, it calls for further investigation. As mentioned earlier, the discrepancy has been interpreted in terms of the increased porosity and the surface roughness effect. Suffice it to mention that actual k_s for the silica powder-filled VIP is roughly one tenth of the upper limit value at $\Pi = 0.26$. The fiber material shows the minimum solid conductivity among the conventional VIP materials. The effective solid conductivity of the staggered beam structure is the lowest, i.e., 0.0009 W/m K. This is the result of the optimized beam sizing. This means that an optimally designed structure having the extended thermal path is the most proper material for the VIP.

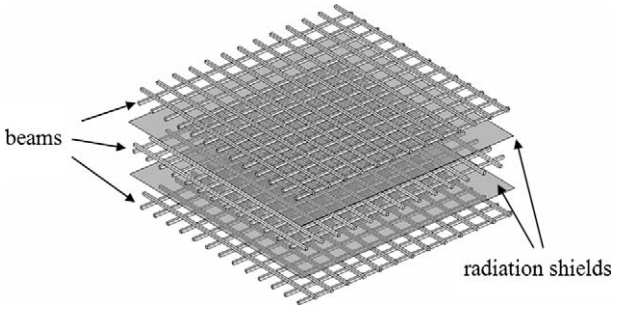

Fig. 7. Multi-layered staggered beam with radiation shields.

Table 1
Thermal conductivities of various core materials for VIPs

	Silica powder		Polyurethane foam	Glass fiber	Polycarbonate staggered beam
Π	0.48	0.26	0.94	0.9	0.84
ρ_s (kg/m^3)	2200		1200	2500	1200
ρ (kg/m^3)	1140	1620	70	250	190
ϕ (μm)	1		100	100	2000
e (m^2/kg)	37	–	44	50	–
k (pure solid conductivity, W/m K)	1.38		0.26	1.3	0.2
k_s (W/m K)	0.0219	0.0634	0.0050	0.0021	0.0009
k_g (W/m K) at 10 Pa	8.12×10^{-6}		7.88×10^{-4}	7.88×10^{-4}	0.015
k_r (W/m K)	0.0002	–	0.0027	0.0007	0.033 (w/o radiation shields) 0.0003 (w/radiation shields)

The gaseous conductivities calculated by using the Smoluchowski model are also presented in Table 1. For 25 ℃ air at 10 Pa, gaseous thermal conductivity of the conventional VIP materials can be neglected due to the very small pore size. The small powder size (few microns) taken in this example, however, may not be practical due to any reason such as health hazard. Greater powder size means increased k_g. The staggered beam is distinctively disadvantageous due to the relatively large pore size comparing to the others. For this reason, the gaseous conductivity of the staggered beam core is recommended to be maintained at a level of 1 Pa to have k_g = 0.0015 W/m K, which is a 'minimum' tolerable pressure to ensure appropriate function as a VIP. The radiative conductivities are shown in Table 1. The results show that the radiative conductivity of the conventional insulations increases with the porosity. The radiation effect in the silica powder insulation can be neglected due to the high solid fraction. In the case of the staggered beam with the multi-layered shields, the radiation effect can also be virtually neglected.

Besides the experimental data of Fricke et al. [11] of $k_{eff} \approx 0.007$ to 0.012 W/m K for silica powder-filled VIP (Π = 0.84), Reuter et al. [30] report for $\Pi \approx 0.91$ as $k_{eff} \approx 0.008$ W/m K. Both are significantly lower than the calculated total conductivity $k_{eff} \approx 0.0219$ (Π = 0.48) to 0.0657 W/m K (Π = 0.26), and it has been mentioned to be due to the increased k_s when using the theoretical models. The total effective conductivity of fiber-filled VIPs (ρ = 240 kg/m^3) made by Owens Corning is about 0.003 W/m K [31]. This agrees fairly well with the calculated result k_{eff} = 0.0036 W/m K (ρ = 250 kg/m^3). Open-celled polyurethane foam (ρ = 60 kg/m^3, ϕ = 100 μm) based VIPs show the total effective conductivity of 0.005–0.007 W/m K at a pressure of 1 Pa [32]. At the same pressure, the calculated one shows as k_{eff} = 0.0078 W/m K, which is in good agreement again with the experiments. The total effective conductivity of the staggered beam with multi-layered radiation shields is given as k_{eff} = 0.0027 W/m K at 1 Pa. This minimum total effective conductivity results from the reduction of both solid conduction effects due to the intentionally extended thermal path and radiation shields. In a recent series of experiment using a guarded hot plate apparatus (GHP 456 Titan, NETZSCH), the effective thermal conductivity of a staggered beam VIP excluding cover plates and envelope is measured to be 0.0026 W/m K, confirming the aforementioned theoretical predictions, although the detailed discussion remained to be published later.

6. Conclusion

Heat transfer mechanisms with powder, foam, fiber and staggered beam as the VIP's filling material have been investigated theoretically. The solid conductivity is obtained using simplified models. The effective solid conductivity is related with the porosity, pure solid conductivity and mechanical properties of the material. The fiber and staggered beam core are recommended in the aspect of the solid conduction due to the tortuously long thermal path. The gaseous conductivity at low pressure is dependent on the pore size and the pressure of the core. The radiative transfer in the various insulation materials is obtained using the diffusion approximation. It depends on the specific extinction coefficient, density and temperature of the core. Based on the separately derived thermal conductivities, the total effective conductivities of VIPs can be predicted accurately except for the packed bed. The proposed analytical tools are useful for further VIP developments. Also, the results show that the fibers and staggered beams with radiation shields are proper filling materials for VIPs.

Acknowledgments

The authors gratefully acknowledge the financial support of several projects: Energy, Environment, Water, and Sustainability (EEWS) program funded by the Korea Advanced Institute of Science and Technology (KAIST), the Brain Korea 21 (BK21) program funded by Ministry of Education, Science and Technology (MEST) and the Manpower Development Program for Energy & Resources funded by the Ministry of Knowledge and Economy (MKE).

References

[1] V.R. Gordon, P.E. Holness, Improving energy efficiency in existing buildings, ASHRAE J. 50 (2008) 12–26.
[2] V. Nemanic, Vacuum insulating panel, Vacuum 46 (1995) 839–842.
[3] G. Kawaguchi, K. Nagai, Vacuum insulation spacer, US Patent No. 4409770, 1983.
[4] J.B. Blackmon, F.C. Wessling, Insulation system having vacuum encased honeycomb offset panels, US Patent No. 20050042416, 2005.
[5] C.K. Chan, C.L. Tien, Conductance of packed spheres in vacuum, ASME J. Heat Transfer 95 (1973) 302–308.
[6] P.J. Turyk, M.M. Yovanovich, Modified effective conductivity models for basic cells of simple cubic packed beds, in: Proceedings of the 23rd National Heat Transfer Conference, Denver, CO, 1984, pp. 9–19.
[7] J. Kuhn, H.P. Ebert, M.C. Arduini-Schuster, D. Buttner, J. Fricke, Thermal transport in polystyrene and polyurethane foam insulations, Int. J. Heat Mass Transfer 35 (1992) 1795–1801.
[8] C. Bankvall, Heat transfer in fibrous materials, J. Test. Eval. 1 (1973) 235–243.
[9] K.L. Johnson, Contact Mechanics, Cambridge University Press, Cambridge, 1985. pp. 84–100.
[10] F.P. Incropera, D.P. Dewitt, Fundamentals of Heat and Mass Transfer, fourth ed., John Wiley & Sons, New York, 1996. pp. 169–171.
[11] J. Fricke, H. Schwab, U. Heinemann, Vacuum insulation panel-exciting thermal properties and most challenging applications, Int. J. Thermophys. 27 (2006) 1123–1139.
[12] T. Rettelbach, J. Sauberlich, S. Korder, J. Fricke, Thermal conductivity of silica powders at temperatures from 10 to 275 K, J. Non-Cryst. Solids 186 (1995) 278–284.
[13] G. Buonanno, A. Carotenuto, G. Giovinco, N. Massarotti, Experimental and theoretical modeling of the effective thermal conductivity of rough steel spheroid packed beds, J. Heat Transfer 125 (2003) 693–702.
[14] M.A. Schuetz, L.R. Glicksman, A basic study of heat transfer through foam insulation, J. Cell. Plast. 20 (1984) 114–121.

[15] J. Fricke, U. Heinemann, H.P. Ebert, Vacuum insulation panel – from research to market, Vacuum 82 (2008) 680–690.
[16] J. Fricke, D. Buttner, R. Caps, J. Gross, O. Nilsson, Solid conductivity of loaded fibrous insulations, Insul. Mater. Test. Appl., ASTM STP1030 (1990) 66–78.
[17] A. Roth, Vacuum Technology, third ed., Elsevier, Amsterdam, 1990. pp. 37-56.
[18] J.M. Lafferty, Foundations of Vacuum Science and Technology, John Wiley & Sons, New York, 1998. pp. 50–51.
[19] E.H. Kennard, Kinetic Theory of Gases with an Introduction to Statistical Mechanics, McGraw-Hill, New York, 1938. pp. 311–318.
[20] T.M. Thomas, Cryogenic Engineering, second ed., Marcel Dekker, New York, 2005. pp. 459–460.
[21] V.A. Petrov, Combined radiation and conduction heat transfer in high temperature fiber thermal insulation, Int. J. Heat Mass Transfer 40 (1997) 2241–2247.
[22] M.F. Modest, Radiative Heat Transfer, second ed., McGraw-Hill, New York, 1993. pp. 451–453.
[23] W.H. Tao, H.C. Hsu, C.C. Chang, C.L. Hsu, Y.S. Lin, Measurement and prediction of thermal conductivity of open cell rigid polyurethane foam, J. Cell. Plast. 37 (2001) 310–332.
[24] R. Caps, A. Trunzer, D. Buttner, J. Fricke, Spectral transmission and reflection properties of high temperature insulation materials, Int. J. Heat Mass Transfer 27 (1984) 1865–1872.
[25] R. Mathes, J. Blumenberg, K. Keller, Radiative heat transfer in insulation with random fibre orientation, Int. J. Heat Mass Transfer 33 (1990) 767–770.
[26] R. Caps, J. Fricke, Thermal conductivity of opacified powder filler materials for vacuum insulations, Int. J. Thermophys. 21 (2000) 445–452.
[27] K.Y. Wang, C.L. Tien, Radiative heat transfer through opacified fibers and powders, J. Quant. Spectrosc. Radiat. Transfer 30 (1983) 213–223.
[28] N.E. Hager, R.C. Steere, Radiant heat transfer in fibrous thermal insulation, J. Appl. Phys. 38 (1967) 4663–4668.
[29] I.S. Yoon, T.H. Song, Thermal conductance of multiple vacuum/plate layer, Thermal Sci. Eng. 13 (2005) 29–32.
[30] R. Reuter, G. Sextl, A.G. Degussa, Vacuum insulation panels (VIPs), in: Non-Fluorocarbon Insulation, Refrigeration and Air-Conditioning Technology Workshop, Wiesbaden, 1993.
[31] R. McGrath, Owens Corning, A fiberglass-based vacuum insulation panel technology, in: Non-Fluorocarbon Insulation, Refrigeration and Air-Conditioning Technology Workshop, Wiesbaden, 1993.
[32] A.J. Hamilton, An evaluation of the practical application and use of VACPAC panel technology, Vuoto scienza et tecnologia 28 (1999) 27–30.